

PPC simulation in string 63 for IceCube Detector

Nianqi Tang (Petra)
Gateway Antarctica
University of Canterbury
Supervisor: Dr Anthony Brown

February 18, 2011

Thanks to Dr Anthony Brown's assistant and support.

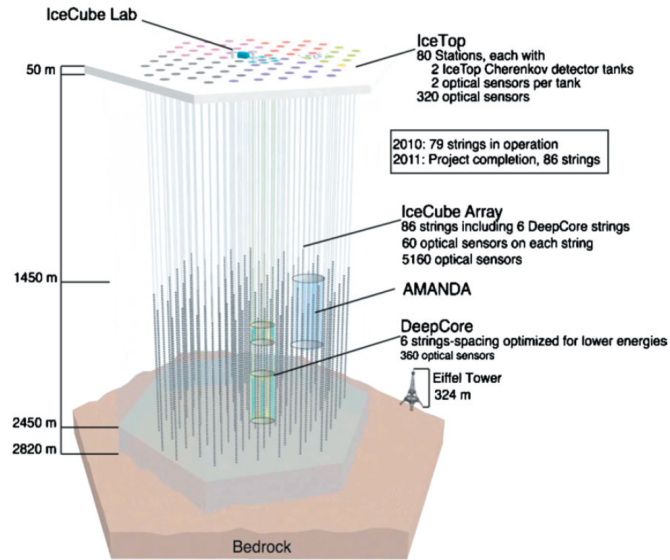


Figure 1: IceCube neutrino observatory. Includes 86 strings, 60 DOMs on each string. Source [1]

Abstract

With the completion of IceCube neutrino observatory in 18th December 2011, scientist will be able to operate the telescope fully in order to solve their curiosities. The study of how light travels between DOMs gives important information to help making models. Because photons can mainly be absorbed or scattered before they hit the detectors, it is essential to understand how these two factors work within the model. This paper will focus on how the variation of scattering length and absorption length change the results of photon detection, some positive results have been found from this study.

Chapter 1

Introduction

The IceCube neutrino observatory is a cubic kilometre neutrino detector completed on the 18th of December 2010 at the geographic South Pole, Antarctica. It is optimized to detect neutrinos over a wide range of energies, from 100 GeV to 10⁹ GeV. The buried array consists of 86 strings inserted in the polar icecap between 1450 m - 2450 m below the surface. Each string consists of 60 digital optical modules (DOMs) (Figure 1). Each DOM comprises a photomultiplier tube, digitising electronics, and light sources for calibration [2] (Figure 1.1).

IceCube is designed primarily to detect high energy neutrinos from astrophysical sources, in order to determine the properties for production (such as α and β particles) of high energy cosmic rays. The properties of light propagation in ice can be described in terms of the average distance between successive scatters (scattering length) and the average distance of absorption (absorption lengths), as well as the angular distribution of the new direction of the photon relative to the previous ones at a given scattering point (this latter will not be discussed in this study). These details are used in many simulations and reconstructions of IceCube data, therefore they are very important and we have to study them to the best possible precision. This report will vary the scattering length (λ_s) and absorption length (λ_a) by using the Photon Propagation Code (PPC), such code propagates photons through heterogeneous ice described by the six-parameter ice model which is based on a selected set of parameters until they hit a DOM or get absorbed [3]. By analysing the outcome data from this study we are able to give interpretations of how varying λ_s and λ_a alone will change the probability density of the photon detection.

Main Aims and Objectives

1. To describe the waveforms and changes in the waveform with an array of variables such as λ_s and λ_a
2. To quantify and interpret the PPC simulation results including total number of detected photon, skewness and kurtosis of the probability density diagrams

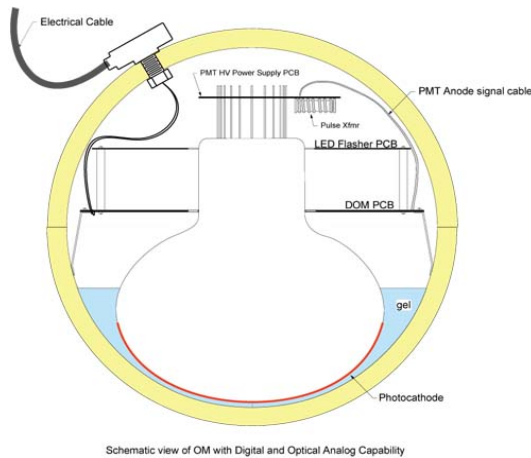


Figure 1.1: Digital Optical Module (DOM). Flasher LEDs are located at the top half hemisphere, detector is located at the bottom half hemisphere

3. To identify the relation of scattering and absorption with respect to the probability density diagrams

Methodology and Setup In this study, we choose string 63 DOM 50 (about 2,300 m below the surface) as our flasher source, shown in Figure 1.2 and 1.3. String 63 is in the middle of the IceCube structure, and DOM 50 is located below dust layer (1250m) and air bubbles in the ice, in this way, the simulation will have a minimum optical impact such as low effective scattering coefficient [4] from the dust particles and residual air bubbles within the ice, since all bubbles have become solid phase at around 1,500 m [5]. We also analyse the two vertically and two horizontally nearest DOMs to the flasher source, they are string 63 DOM 49, string 63 DOM 51, string 62 DOM 50 and string 64 DOM 50 (Figure 1.3). Each flashing is capable of emitting 10^9 photons in nanosecond scale, if a receiver recorded more than one photon in an event, only the earliest time was retained.

Firstly, we will record the probability densities of photon detection vertically in string 63 DOM 49 and DOM 51, and horizontally in string 62 DOM 50 and string 64 DOM 50, then compare the results.

Secondly, we will vary λ_s by 10% and 20% then record the probability densities at the same DOMs, quantify the outcome and compare the data with the first set of data.

Lastly, we will vary λ_a by 10% and 20% respectively and follow by the similar analysis method as above.

All calculations and diagrams are done by MATLAB.

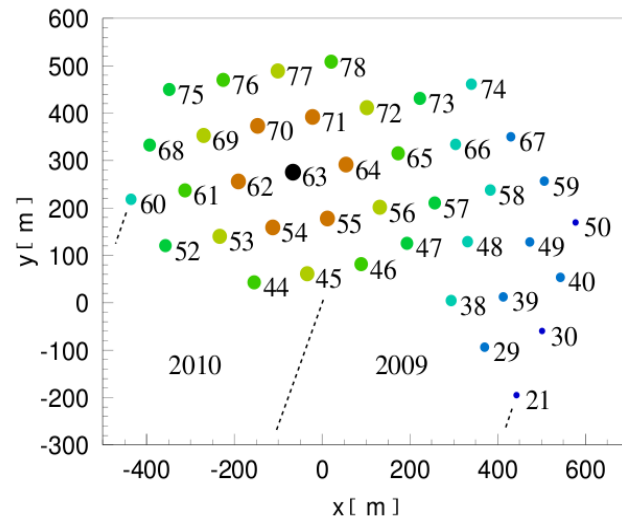


Figure 1.2: IceCube String Profile from the surface. 40 coloured dots indicate strings with position numbers next to them, where the black dot indicates the location of the LEDs flasher in this study. 2009 and 2010 indicate the year of completing of string installation. Both axis indicate the distance away from the centre of IceCube

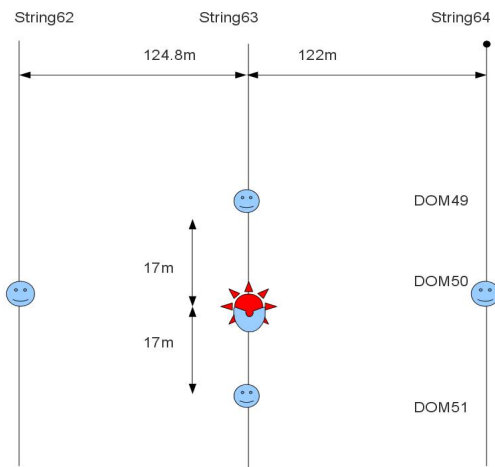


Figure 1.3: Flasher event in this study. Red in the centre represents the LED flashers, smiley faces represent DOMs, vertical lines represent strings, arrowed lines represent distances in metres, diagram is not in scale

Chapter 2

Vertical and Horizontal Comparision in String 63

Model PPC simulates a flasher emitting 10^9 photons. LEDs flasher location is at string 63 and DOM 50, program compiles the PPC executable for CPU in this study.

Aim Without changing λ_s and λ_a we will investigate how distance between DOMs and thier structures relate to the probability diagrams of detected photons.

Results In Table 5.1 both string 62 DOM 50 and string 64 DOM 50 have similar received numbers of photon, skewness and kurtosis respectively. The probability density diagrams show a similar trend (Figure 2.2), the red lines in the diagrams indicate the tangent lines, which are consistent in the both diagrams. To be notice, photons arrive at horizontal DOMs after 500 ns.

On the other hand, vertical DOMs receive photons much earlier than horizontal DOMs. String 63 DOM 49 receives at least three times more photons than that of in string 63 DOM 51. The probability density diagrams shown a steady drop in DOM 49 but a graduate drop at DOM 51 (Figure 2.3), in DOM 49 there are also higher skewness and kurtosis than in DOM 51 (Table 5.1).

All four probability diagrams skew to the right, the distributions show that the masses of mean are on the left of the symmetrical centre.

Discussion The skewness of all four probability density diagrams indicate that the four DOMs receive more photons without scattering than photons after scattering in each simulation, and the scatterings occur even after 2,500 ns, String 62 DOM 50 and string 64 DOM 50 receive photon much later (>500 ns) and thicker tails than that of in string 63 DOM 49 and string 63 DOM 51, this is due to the distances from string 62 DOM 50 and string 64 DOM 50 are great than that of other two (Figure 1.3), it takes photons longer to travle greater distance and also there are more chance of scattering on the way.

Because of the similar distances and orientations, string 62 DOM 50 and string 64 DOM 50 share similar probability density distribution (Figure 2.2). However, string 63 DOM 49 and string 63 DOM 51 have different probability density distributions (Figure 2.3), this is because the structure of the DOM (Figure 1.1), the detector is at the bottom half of each DOM and the LEDs flasher are at the top half of string 63 DOM 50. In order to reach the detector at DOM 51, photons have to be scattered first.

In summary, the variation of different DOMs is mostly due to variations in relative orientation of the flasher LEDs with respect to the surrounding strings, emitted photons cannot reach DOM 51 directly without scattering, therefore DOM 51 diagram has a thicker tail than DOM 49 diagram has. The results may also due to relative variation of light yield between the different flasher LEDs, some differences in distance to and depth of the surrounding strings, and shadowing effect of the cables around the DOMs.

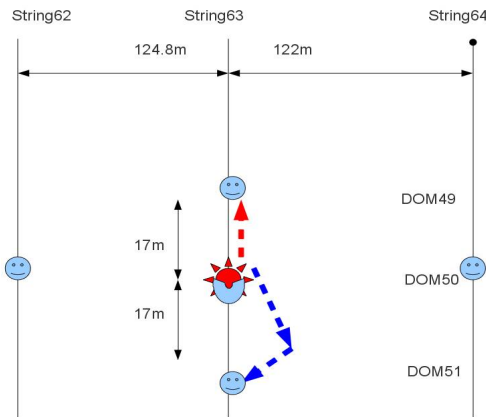


Figure 2.1: Wavefront propagation. Red in the centre represents the LED flashers, smiley faces represent DOMs, vertical lines represent strings, arrowed lines represent distances in metres. Red dotted arrows represents direct detection and the path of photons without scattering, blue represents detection and path of photons with scattering, diagram is not in scale

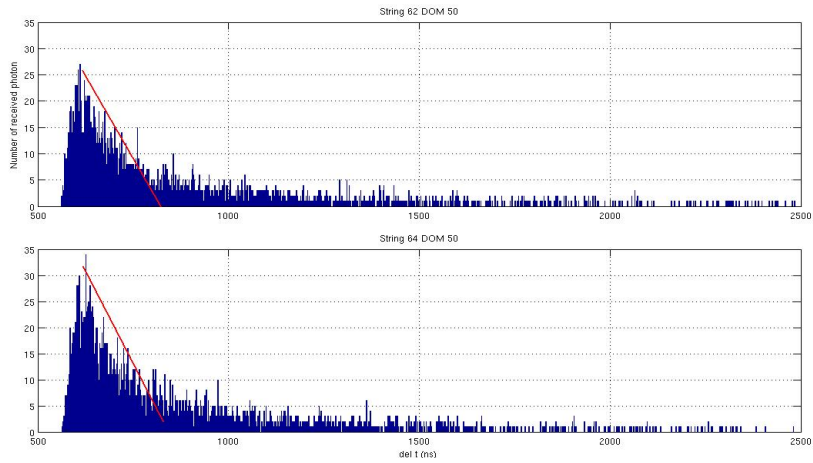


Figure 2.2: Top: probability density diagram of string 62 DOM 50, bottom: probability density diagram of string 64 DOM 50. Red lines represent tangent lines, horizontal axis represents time taken to receive photons in nanoseconds, vertical axis represents number of hits

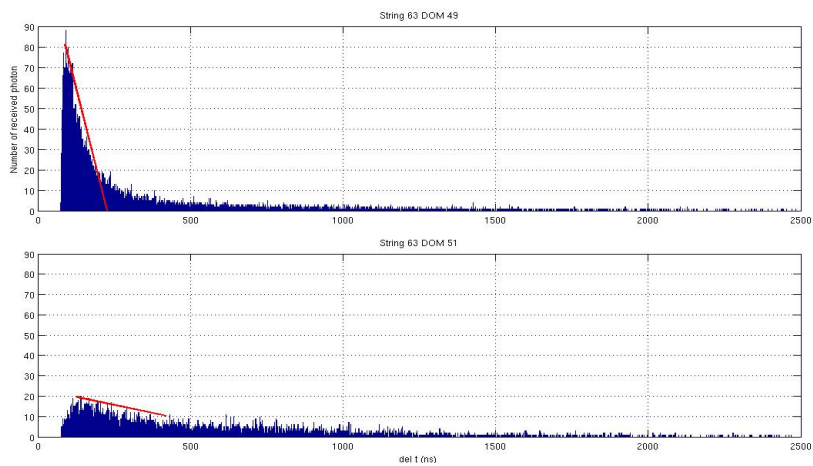


Figure 2.3: Top: probability density diagram of string 63 DOM 49, bottom: probability density diagram of string 63 DOM 51

Chapter 3

Different Scattering Length Comparison

Model PPC simulates a flasher emitting 10^9 photons, with changing of λ_s by 10% and 20%. String 63 DOM 49 is chosen as our study subject in this section because it receives the maximum number of emitted photons (table 1), and it has the closest detection range to LEDs flashers (Figure 1.3). In this way, we will receive maximum information from the simulation.

Aim To quantify the outcome with variation of parameters, and determine how varying λ_s affects the results.

Results The areas of probability diagrams decrease with increasing percentage of λ_s and the tangents drop with increasing percentage of λ_s (Figure 3.1 and Figure 3.2). To be noticed that photons arrive at string 63 DOM 49 at similar times in four cases, -20% λ_s , -10% λ_s , +10% λ_s and +20%.

Figure 4.3 shows a positive linear trend, as the λ_s increases the number of photons detected increases too.

The skewness decreases with increasing λ_s in the four cases, however, the skewness is low in the four cases compared with the simulation without changing in λ_s and λ_a (Figure 4.4). This means that the masses of distribution in the four cases have been shifted slightly to the right of the probability density diagrams after changing of λ_s .

Figure 4.5, the kurtosis drops dramatically from varied λ_s of -20% to -10%, then it decreases gradually with increasing λ_s . To be noticed, changing of λ_s decreases kurtosis, which means that the peak value of probability density diagram is the highest in the simulation without any change in λ_s .

Discussion Results find that the number of detected photons is proportional to λ_s , this means that emitted photons have a better chance to reach the detectors before they get scattered away with longer λ_s . Low skewness value indicates a more symmetrical probability distribution, which

means that with increasing λ_s , the masses of distribution shift to the right of the diagram, as a result, we observe an increasing percentage of photon scattering within each simulation.

A similar result also apply to kurtosis with increasing λ_s . The general trend of kurtosis decreases with increasing λ_s . This can be explained as when we increase λ_s the less chance to detect photons at the same time, this confirm the result that as we increase the λ_s , we also see increase the number of photon scattering. To be notice that changes of λ_s decreases the kurtosis value. Low kurtosis indicates more variance, which is the result of infrequent extreme deviations, this means that photon detection reaches its critical skewness and kurtosis values without any change of λ_s .

Moreover, the steady drop of kurtosis from no change in λ_s to -20% λ_s and then to -10% λ_s (Figure 4.5) give us an range of how much λ_s we can increase until we cannot take its value into account in the IceCube model any more, more data and investigation are needed to answer this question.

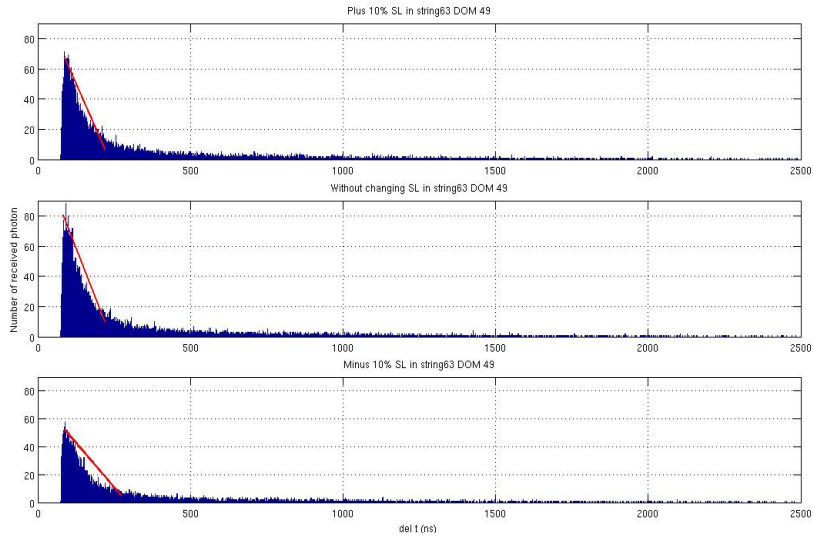


Figure 3.1: Within string 63 DOM 49, Top: probability density diagram of varying $+10\%$ λ_s , middle: probability density diagram without varying λ_s and λ_a , bottom: probability density diagram of varying -10% λ_s

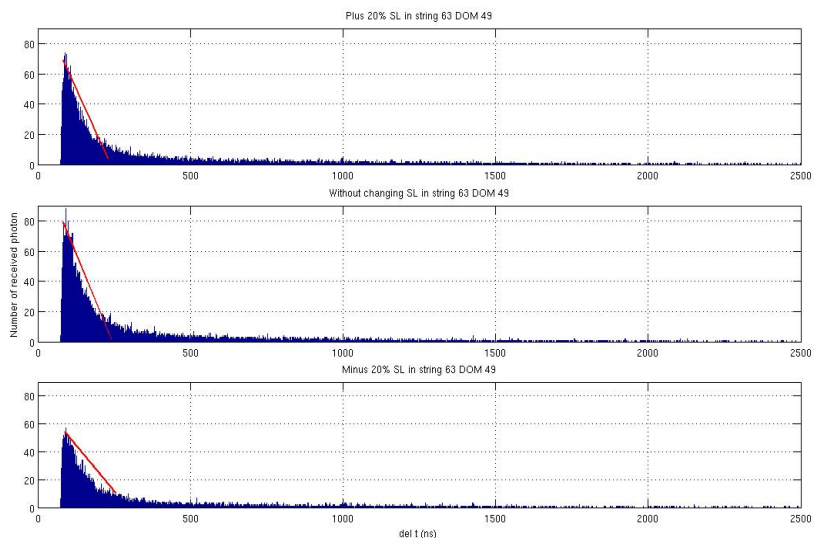


Figure 3.2: Within string 63 DOM 49, Top: probability density diagram of varying +20% λ_s , middle: probability density diagram without varying λ_s and λ_a , bottom: probability density diagram of varying -20% λ_s

Chapter 4

Different Absorption Length Comparison

Model PPC simulates a flasher emitting 10^9 photons, with changing of λ_a by 10% and 20%, again we choose string 63 DOM 49 as our study subject.

Aim To quantify the outcome with variation of parameters, and determine how varying λ_a effect the results.

Results The areas of probability diagrams cover decrease slightly with increasing percentage of λ_a and the tangents drop also slightly with increasing percentage of λ_s (Figure 3.1 and Figure 3.2). To be notice that photons arrive at string 63 DOM 49 at similar times in four cases, -20% λ_a , -10% λ_a , +10% λ_a and +20%.

Figure 4.3 shows a negative linear trend, as the λ_a increases the number of photon been detectd decrease slightly.

The skewness decreases with changing λ_a , the values in the four DOMs are all just below 3, which is lower compare with the simulation without changing in λ_s and λ_a (Figure 4.4), at +10% λ_a the skewness is the lowest. The decreasing skewness means that the masses of distribution in the four cases have been shifted slightly to the right of the probability density diagrams after changing of λ_a .

Figure 4.5, the kurtosis drops dramatically from varied λ_s of -20%, then it decreases gradually with increasing λ_s until +10% of λ_a , followed by an increasing kurtosis value at +20% of λ_a . To be notice, changing of λ_a decreases kurtosis, which means that the peak value of probability density diagram is the highest in the simulation without any change in λ_s .

In summery, the probability density diagrams, skewness and kurtosis of the four detection DOMs are alike (Figure 4.1, Figure 4.2, Figure 4.4 and Figure 4.5).

Discussion Results find that number of detectd photon proportional to the inverse of λ_a , a general increasing tangent lines with increasing λ_a means that emitted photons have less chance to get scattered before they reach the detectors

with increasing λ_a . Low skewness value indicates a more symmetrical probability distribution, with varying λ_a , the masses of distribution shift to the right of the diagram, as a result, we observe an decreasing percentage of photon scattering within each simulation.

The general trend of kurtosis keeps constant with varying λ_a . With increasing λ_a , there is a slight more chance to detect photons at the same time, this confirm with the result that as we increase the λ_a , we also see a slight decreasing number of photon scattering. To be notice the result without changing of λ_s and λ_a has the maximum number of photon scattering. Similar to varying λ_s simulation, low kurtosis indicates more variance, which is the result of infrequent extreme deviations, this means that photon detection reaches its critical skewness and kurtosis values without any change of λ_a .

In conclusion, the effect of varying λ_a is not as obvious at varying λ_s in this study, more information is needed to explain the variations.

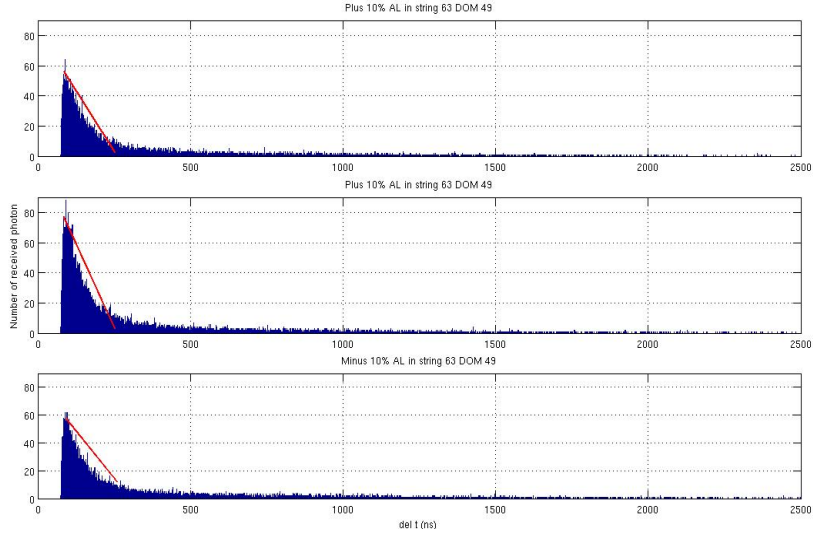


Figure 4.1: Within string 63 DOM 49, Top: probability density diagram of varying +10% λ_a , middle: probability density diagram without varying λ_s and λ_a , bottom: probability density diagram of varying -10% λ_a

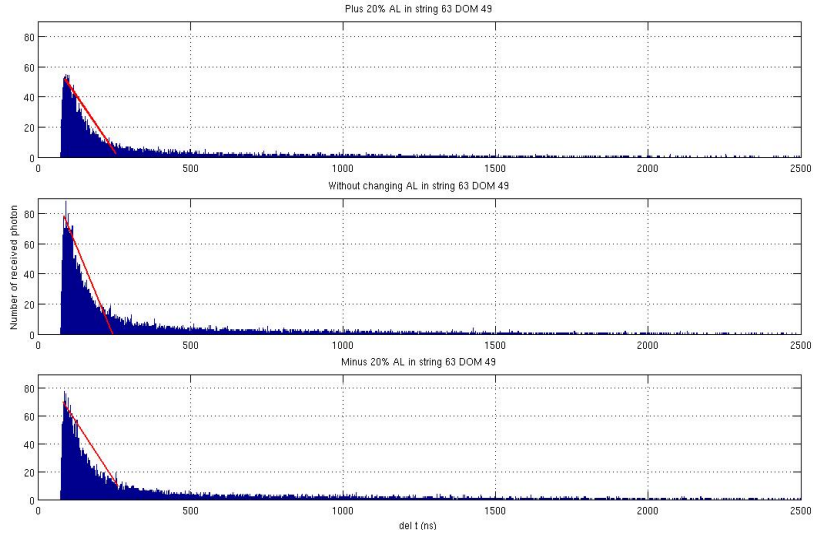


Figure 4.2: Within string 63 DOM 49, Top: probability density diagram of varying +20% λ_s , middle: probability density diagram without varying λ_s and λ_a , bottom: probability density diagram of varying -20% λ_s

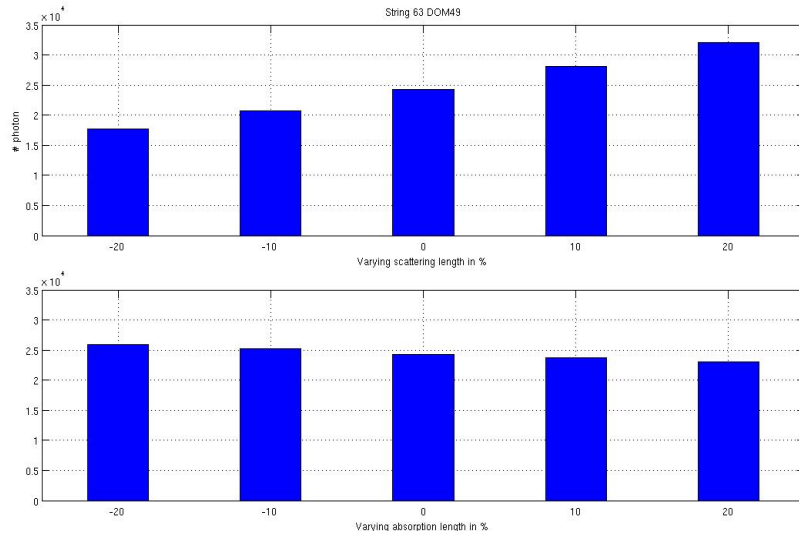


Figure 4.3: Top: number of photon received with different λ_s , bottom: number of photon with different λ_a . Horizontal axis represents changes in percentage, top for λ_s bottom for λ_a . Vertical axis represents number of photons received

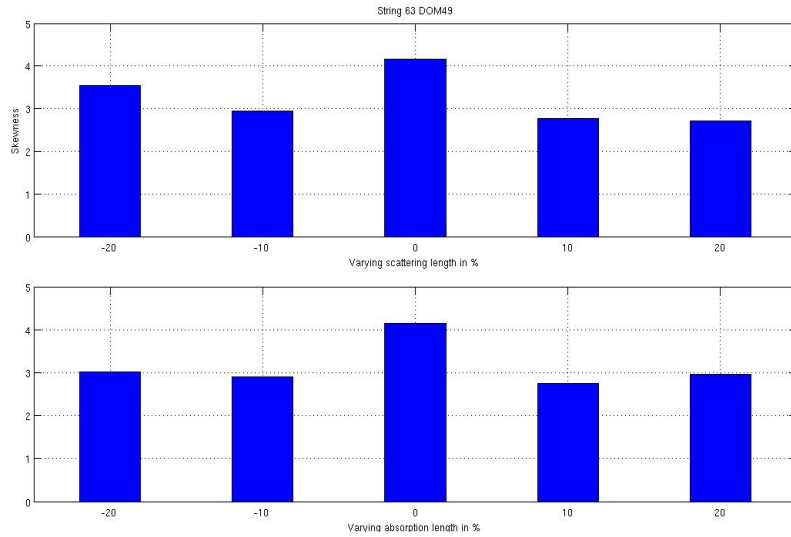


Figure 4.4: Top: skewness of different λ_s , bottom: skewness of different λ_a . Horizontal axis represents changes in percentage, top for λ_s bottom for λ_a . Vertical axis represents skewness

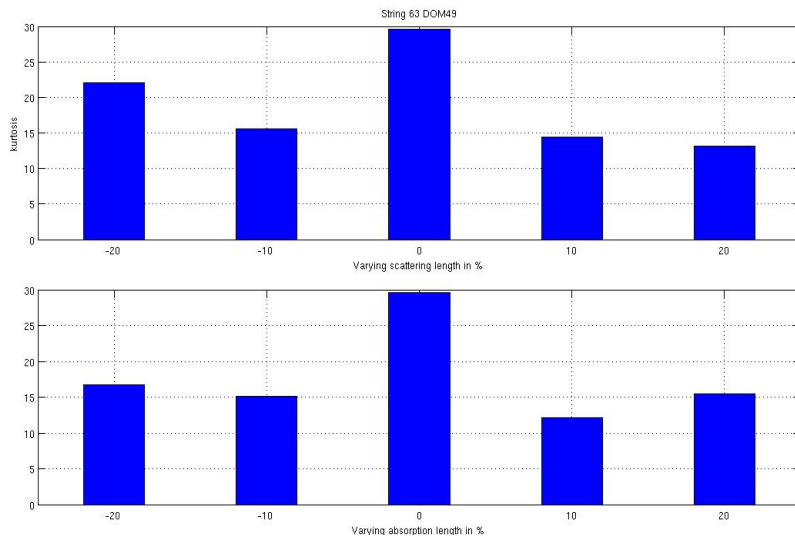


Figure 4.5: Top: kurtosis of different λ_s , bottom: kurtosis of different λ_a . Horizontal axis represents changes in percentage, top for λ_s bottom for λ_a . Vertical axis represents kurtosis

Chapter 5

Conclusion

A better understanding of the structure of different DOMs and how light propagate between the DOMs is crucial in the study of IceCube projects, this is because of the variations in relative orientation of the flasher LEDs with respect to the surrounding strings and the devices attached to the DOMs all effect the quality and quantity of received photons.

Whether or not a photon is scattered before it reaches the DOMs is hugely depends on the λ_s and the distance of the journey. With the help of mathematical explanations, we are able to tell that the probability density of detected photons is driven mainly by an range of λ_s , this study only show a little evidence of impact of different λ_a on the probability density distributions of detected photons. All in all, the results of this study can be described as follow:

$$n \propto \lambda_s \propto \frac{1}{\lambda_a}$$

$$skewness \propto \frac{1}{\lambda_s}$$

$$kurtosis \propto \lambda_s$$

Where n is number of detected photons.

However, there are many exceptions in comparing kurtosis with other parameters, we can not draw a solid conclusion of how varying λ_s and λ_a effect kurtosis. The uncertainty of choosing string 63 DOM 49 as our study subject may be big, this is due to its location to the LEDs flasher, it may not review the general properties of the probability density of the received photons. More testing and DOMs needed to give more general conclusion to this study.

Table 5.1: Results

	63DOM49	63DOM51	62DOM50	64DOM50
Without changing				
Received photon	24249	7095	3168	3350
Skewness	4.1552	2.2114	3.015	2.964
Kurtosis	29.6005	11.3548	15.9887	16.3071
Plus 10% λ_s				
Received photon	28154	8349	3055	3231
Skewness	2.7650	2.6925	4.1484	2.2707
Kurtosis	14.4681	13.6802	29.1236	11.5798
Minus 10% λ_s				
Received photon	20756	5573	3272	3376
Skewness	2.9492	3.1617	4.0839	2.2101
Kurtosis	15.6159	17.6811	25.5133	10.6122
Plus 20% λ_s				
Received photon	32116	10008	3060	3114
Skewness	2.709	2.4894	3.9488	2.0297
Kurtosis	13.1951	11.9016	25.1562	8.9787
Minus 20% λ_s				
Received photon	17655	4421	3331	3454
Skewness	3.5443	3.1765	4.0735	2.6914
Kurtosis	22.0087	16.1361	25.4745	20.5609
Plus 10% λ_a				
Received photon	23680	6568	2923	3042
Skewness	2.7565	3.3483	4.0339	2.0519
Kurtosis	12.0727	20.6863	26.2815	8.8957
Minus 10% λ_a				
Received photon	25206	7470	3500	3646
Skewness	2.9082	2.7333	3.9886	2.8741
Kurtosis	15.0665	13.0857	25.9263	19.5925
Plus 20% λ_a				
Received photon	23093	6230	2722	2913
Skewness	2.9575	2.6702	4.0749	2.1253
Kurtosis	15.4506	13.1422	25.5514	9.6291
Minus 20% λ_a				
Received photon	25918	7755	3832	4055
Skewness	3.009	2.8377	4.1206	2.5173
Kurtosis	16.7008	14.1985	27.6824	15.8209

References

1. Brown, A. M. 2010. Latest results from IceCube Experiment. *IceCube Collaboration*, University of Canterbury, New Zealand
2. <http://internal.icecube.wisc.edu>
3. Chirkin, D. 2008, Study of South Pole ice transparency with IceCube flashers. University of Wisconsin, Madison, USA
4. Whitehead, S. R. 2008, On the Properties of Ice at the IceCube Neutrino Telescope, *A thesis submitted in partical fulfilment of the requirements for the degree of Master of Science*, University of Canterbury, New Zealand
5. Price PB. Optical properties of deep glacial ice at the South Pole. *Journal of geophysical research*. Biogeosciences. 2006-07-08;111:D13203.